Molecular BioSystems

RSC Publishing

PAPER

View Article Online
View Journal | View Issue

Cite this: *Mol. BioSyst.*, 2013, **9**, 3117

Effects of temperature on the dynamics of the LacI-TetR-CI repressilator

Jerome G. Chandraseelan, Samuel M. D. Oliveira, Antti Häkkinen, Huy Tran, Ilya Potapov, Adrien Sala, Meenakshisundaram Kandhavelu and Andre S. Ribeiro*

Received 31st May 2013,
Accepted 27th September 2013

DOI: 10.1039/c3mb70203k

www.rsc.org/molecularbiosystems

We studied the behaviour of the repressilator at 28 °C, 30 °C, 33 °C, and 37 °C. From the fluorescence in each cell over time, we determined the period of oscillations, the functionality (fraction of cells exhibiting oscillations) and the robustness (fraction of expected oscillations that occur) of this circuit. We show that the oscillatory dynamics differs with temperature. Functionality is maximized at 30 °C. Robustness decreases beyond 30 °C, as most cells exhibit 'failed' oscillations. These failures cause the distribution of periods to become bimodal, with an 'apparent period' that is minimal at 30 °C, while the true period decreases with increasing temperature. Based on previous studies, we hypothesized that the failures are due to a loss of functionality of one protein of the repressilator, CI. To test this, we studied the kinetics of a genetic switch, formed by the proteins CI and Cro, whose expression is controlled by P_{RM} and P_R, respectively. By probing the activity of P_{RM} by *in vivo* detection of MS2-GFP tagged RNA, we find that, beyond 30 °C, the production of the CI-coding RNA changes from sub-Poissonian to super-Poissonian. Given this, we suggest that the decrease in efficiency of CI as a repressor with temperature hinders the robustness of the repressilator beyond 30 °C. We conclude that the repressilator is sensitive but not robust to temperature. Replacing CI for a less temperature-dependent protein should enhance robustness.

Introduction

Natural genetic circuits can efficiently perform various tasks, such as time counting,[1] state holding,[2] and signal filtering,[3] while maintaining robustness to environmental changes. This is necessary for them to be able to regulate complex cellular processes under various conditions[4–6] or to efficiently determine cells' response to environmental shifts and signals. Much effort has been made to reproduce their behaviour in synthetic circuits.[6–8] Once proven reliable, these synthetic circuits should have a wide range of applications.[9–12] For example, synthetic genetic clocks promise to be of use as regulators of intracellular processes. For that, they will need to be robust to environmental changes, similarly to natural circuits.

One of the most famous synthetic circuits is the 'repressilator', engineered by Elowitz *et al.*[7] This circuit has three genes, whose interactions form a negative feedback loop. Namely, the three genes form a cycle, with each gene expressing a protein that represses the next gene in the cycle. At 30 °C, the repressilator exhibits periodic oscillations,[7] visible in time-lapse measurements of a green fluorescent protein (GFP) reporter that is under the control of a promoter that is also present in the 3-gene circuit.

Temperature affects the dynamics of most cellular processes, including gene expression.[13] Evidence suggests that natural, time-keeping circuits, such as circadian oscillators, evolved robustness to temperature fluctuations.[14–16] Similar robustness is desired in synthetic circuits designed for time keeping.

The degree of robustness of the repressilator to temperature is unknown, but studies on some of its components suggest that its behaviour is bound to be strongly affected by small changes in temperature. For example, one of its proteins, the wild-type CI,[7] has temperature-dependent DNA-binding stability.[17] Namely, it is maximized at ~30 °C and is gradually lost as temperature increases, becoming ~50% weaker at 42 °C.[17] This decrease may arise from the fact that the ability of CI to discriminate between operator sites depends on ion binding/release reactions[18] and/or from the temperature-dependence of the CI's dimerization process.[19]

Here, we investigate how temperature affects the dynamics of the repressilator. Afterwards, we search for causes. Motivated by previous evidence that CI's functionality is temperature-dependent, we also study the temperature-dependence of another circuit, the CI–Cro switch. After comparing the effects of temperature on the kinetics of the two circuits, we propose

Computational Systems Biology Research Group, Tampere University of Technology, P.O. Box 553, 33101 Tampere, Finland. E-mail: andre.ribeiro@tut.fi

modifications to the repressilator that may enhance its robustness to temperature fluctuations.

Methods

Repressilator: strain, plasmid, and microscopy

Cells of *E. coli* lac$^-$ strain MC 4100 with the repressilator (pZS1-lTlrLLtCL) and the reporter plasmid (pZE21-GFPaav) were generously provided by M. Elowitz, Princeton University, NJ, USA. Minimal media were prepared with 2 mM $MgSO_4 \cdot 7H_2O$ (Sigma-Aldrich, USA), 7.6 mM $(NH_4)_2SO_4$ (Sigma Life Science, USA), 30 μM $FeSO_4 \cdot 7H_2O$ (Sigma Life Science, USA), 1 mM EDTA (Sigma Life Science, USA), 60 mM KH_2PO_4 (Sigma Life Science, USA) pH 6.8 with Glycerol 0.5% (Sigma Life Science, USA) and Casaminoacids 0.1% (Fluka Analytical, USA).

E. coli cells with the repressilator and reporter plasmids were grown in minimal media overnight at 28 °C, 30 °C, 33 °C or 37 °C with shaking at 300 rpm, to an optical density (OD) of 0.1 at 600 nm. Next, cells were diluted into fresh media and a few μl of the culture was placed between a cover-slip and a slab of 2% low melting agarose in minimal media, 0.75 mm thick. During time lapse microscopy, the temperature of the samples was kept stable by a control chamber (Bioptechs, FCS2, Pennsylvania, USA). Images were obtained every 15 minutes for 10 hours by a Nikon Eclipse (TE2000-U, Nikon, Tokyo, Japan) inverted C1 confocal laser-scanning system with a 100× Apo TIRF (1.49 NA, oil) objective. GFP fluorescence was measured using a 488 nm laser (Melles-Griot) and a 515/30 nm detection filter. For image acquisition, we used Nikon software EZ-C1.

Switch: strain, plasmid, and microscopy

E. coli CZ071 with a reporter plasmid PLtetO-1-MS2d-GFP and a target plasmid pIG-BAC (P_{RM}-limm(rexAB::bs48)) were generously provided by I. Golding (University of Illinois, USA). The target plasmid is a single-copy F-plasmid with a genetic switch coding for CI, under the control of P_{RM}, and Cro,[20] under the control of P_R. Further, the plasmid contains the immunity region of wild-type λ,[21] where the rexA and rexB genes were replaced by a 48 binding site array for MS2d proteins, so as to detect individual RNAs whose production is controlled by P_{RM}. Depending on the occupation of the sites OR1, OR2 and OR3, one of the two promoters will be in a repressed state.[32,33] Note that OR3 is absent in the repressilator. Nevertheless, the existence of oscillations[7] shows that CI still achieves repression of P_R.

Cells were grown in Luria–Bertani (LB) medium with the following components: 10 g L^{-1} of Tryptone (Sigma Aldrich, USA), 5 g L^{-1} of yeast extract (LabM, UK) and 10 g L^{-1} of NaCl (LabM, UK), with addition of 34 μg ml^{-1} of Kanamycin and 34 μg ml^{-1} of Chloramphenicol (both antibiotics from Sigma Aldrich, USA). Cells were grown overnight with shaking at 260 rpm, in an orbital shaker (Labnet), at 30 °C for 12–16 h to an optical density (OD) of 0.1 at 600 nm. Thereafter, cells were grown until they reached an OD of ≈0.01 and diluted to 1 : 10 in LB medium with antibiotics. Then, they were grown at 37 °C with shaking at 260 rpm for a few hours, until they reached the exponential phase and an OD of ≈0.3.

The reporter gene, TetO1-MS2d, was activated using 10 ng ml^{-1} of anhydrotetracycline (aTc) (IBA GmbH, Germany), for at least 45 minutes, to allow the production and maturation of enough reporter MS2-GFP proteins. For acclimatization, cells were grown at room temperature for 1 hour. Afterwards, they were transferred to a microscope chamber, for image acquisition.

Cells were kept at 24 °C, 27 °C, 30 °C, 34 °C, or 37 °C during microscopy in a thermal chamber (Bioptechs, FCS2, Pennsylvania, USA). We poured 100 μl of melted agarose-medium with 1% agarose (Sigma life science, USA), LB medium, and aTc (10 ng ml^{-1}), into a microscope slide with a glass coverslip on top. After waiting for the gel-pad to solidify, prior to adding cells, we removed the coverslip and left the gel-pad to dry for 2–5 minutes at room temperature. Finally, we added 5–8 μl of cell suspension into the gel and placed this sandwich in the thermal chamber for image acquisition.

Cells were visualized in a Nikon Eclipse (TE2000-U, Nikon, Japan) inverted microscope with C1 confocal laser-scanning and a 100× Apo TIRF objective. Images were taken every minute for 2 hours. GFP fluorescence was measured using 488 nm argon ion laser (Melles-Griot) and a 515/30 nm emission filter. Images were acquired with Nikon EZ-C1 software and were analysed by custom software written in MATLAB 2011b (MathWorks).

Image analysis

Images of cells with the repressilator and with the switch were analysed differently. To detect cells with the repressilator from images (Fig. 1), we segment them by manually masking the area each occupies in each frame. Next, the total fluorescence intensity in each mask is extracted and the mean pixel intensity of each cell is calculated for each time moment.

For cells containing the switch, thus expressing MS2-GFP and its target RNA, the region occupied by each cell over time was manually masked. In each mask, principal component analysis (PCA) was used to obtain dimensions and orientation of the cell at each moment. By kernel density estimation using a Gaussian kernel[22] and Otsu's thresholding,[23] fluorescent spots were automatically segmented. To obtain the intensity of each spot, the cell background was subtracted. Finally, RNA numbers in each cell were obtained from the time series of the corrected total spot intensity by a least squares fit of a monotone piecewise-constant curve (Fig. 2b).[24] The number of terms in the curve was selected by an *F*-test with a *p*-value of 0.01. Each jump corresponds to the production of one RNA[24] (Fig. 2, for details see ref. 25).

Assessing functionality and apparent period of oscillations

To determine if a repressilator is 'functional' during a time series, we use the criterion used in Elowitz *et al.*[7] A fast Fourier transform is applied to the temporal fluorescence signal from

Fig. 1 Cell exhibiting oscillatory fluorescence. 5 frames are shown, along with time stamps in minutes. In this case, the images were taken at 30 °C.

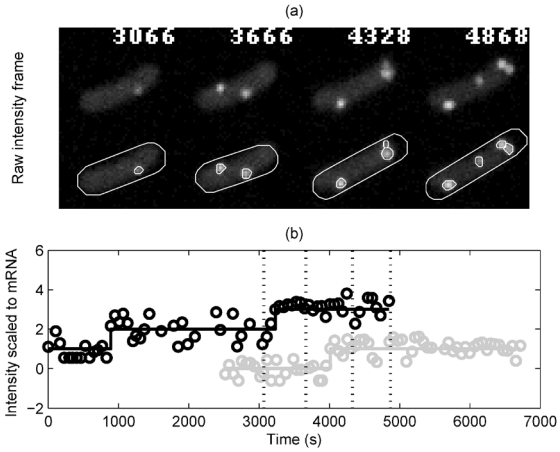

Fig. 2 MS2-GFP tagged RNAs in *E. coli* cells. Unprocessed and segmented cells and RNA spots (a). Moments when images were taken are indicated in each frame. Examples of time series in cells with scaled intensity levels (circles) and estimated RNA numbers (solid lines) (b).

each cell and divided by the transform of a decaying exponential with a time constant of 90 min, the measured lifetime of the fluorescent protein used (GFPaav).[7] Power spectra with peaks 4.5 times higher than the background at frequencies of 0.15–0.5 per hour were classified as oscillatory. The bandwidth used here is larger than in ref. 7 so as to include failed oscillations that should cause apparent oscillations with close to double period.

For cells considered functional, we estimated the 'apparent period' as follows. First, we fit a quadratic curve in the least-squares sense to the intensity time series, to estimate the general trend (Fig. 3, top panel) since the measured intensity is affected by, *e.g.*, photo-bleaching. After subtracting the estimated trend, the residual is scaled to unit power (Fig. 3, middle panel), and then the autocorrelation function is computed (Fig. 3, bottom panel). From this function, we estimate the period by locating the first and the third zeros of the autocorrelation function and computing their distance (Fig. 3, bottom panel, black circles).

Detecting failed oscillations and estimating the true period

The above method of period estimation relies on robust periodic behaviours. If a repressilator halts its activity for a while and then resumes it, the above method cannot detect it. Instead, it assumes an oscillation length that includes the halting and the 'true' oscillation. We observed by inspection that, in some cells, the GFP reporter failed to report an oscillation, either because the oscillation itself failed or because the reporters' expression failed. In general, the reporter signal 'recovered' in the next cycle. In these cases, the measured time was double that between other consecutive oscillations.

To extract the 'true period', we employed a method that relies on the fact that the distributions of period lengths, when failures occur, resemble bimodal distributions. Namely, we estimate the mean and standard deviation of the true period in the population and the fraction of failed oscillations from

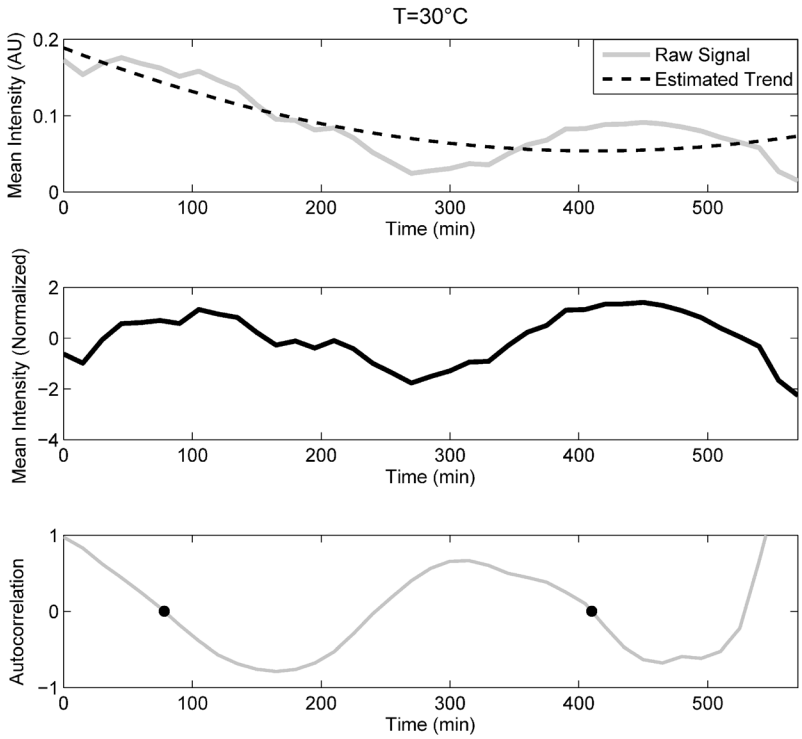

Fig. 3 Period estimation from the fluorescence intensity signal. In the top panel, the raw signal extracted from images is shown along with the estimated trend. In the middle panel, the trend was subtracted from the raw signal and the residual was scaled to unit power. The bottom panel shows the autocorrelation function of the treated signal. The distance between first and third zeros (black circles) corresponds to the period of oscillation in the cell.

the measured periods from each cell. For that, we find the maximum likelihood estimates for a single Gaussian (given by the mean and standard deviation of the measured periods) and for a mixture of two Gaussians, such that the mean and variance of the second are double that of the first (found using an iterative expectation maximization algorithm).[26] The appropriate model is selected by a likelihood ratio test with significance level of 0.01 between the two models. That is, we only select the 2-Gaussian model if the p-value of this test is smaller than 0.01. Finally, we performed the fitting with each subset of data lacking one of the measured periods (leave-one-out technique). This procedure results in N estimates each using $N-1$ measured periods from which the variance of the estimates is estimated.

Results

We measured the behaviour of the repressilator at 28 °C, 30 °C, 33 °C, and 37 °C. We also conducted measurements for lower and higher temperatures than these, but the number of functional repressilators was negligible or non-existing. We limited the measurements' length to 10 h, as cells tend to enter the stationary phase beyond this point, which halts the repressilator.[7] Cells with a non-functional repressilator, for this or other reasons, were discarded by the method used to determine if the GFP levels oscillate throughout the measurement period (see Methods).

We first tested if the distributions of lengths of the oscillations (Fig. 4) here referred to loosely as 'periods', differ with temperature. For that, we compared all pairs of distributions using the Kolmogorov–Smirnov (KS) test. All, except 33 °C *vs.* 37 °C, differ in a statistical sense (p-values smaller than 0.03), which implies that the circuit is sensitive to temperature.

Under all conditions, as visible from the distributions in Fig. 4, the period lengths vary widely. Given their mean and variability, a number of short-lasting periods (<100 min) are expected (visible in Fig. 4). To verify that these did not occur in a higher than expected frequency, for the condition '30 °C' (the one with most samples), we computed the probability of having such or a more extreme number of periods smaller than 100 min (*i.e.* a p-value) assuming the fitted model (see below and the Methods section). From the model, 2.93 'short periods' are expected while 3 were detected, which results in a p-value of 0.56 *i.e.*, the number of events observed is not unlikely.

The effects of temperature on the distribution of periods' length are visible in Fig. 4. The distribution appears to become bimodal for $T > 30$ °C. This bimodality, not possible if the oscillations in protein numbers were robust, appears to arise from 'failed oscillations' that occur with non-negligible probability. Namely, in some of the cells at $T > 30$ °C, the GFP levels appear to remain low for approximately one cycle and only increase again in the following cycle.

To test for bimodality, for each of the four distributions, we determined the maximum likelihood estimates for a single Gaussian and for a mixture of two Gaussians with the mean and variance of the second Gaussian being double those of the first. The preferred model (see Methods) in each condition is shown in Fig. 4 as well. For 33 °C and 37 °C, the model of two Gaussians was preferred.

Using the fitting, we estimated the number of failed oscillations in each cell, under each condition (see Methods). The fraction of successful oscillations (R) is shown in Table 1, for each condition. Beyond 30 °C, the repressilator loses much of its robustness, as several expected oscillations were not detected. This agrees with the observed decrease in functionality (F) for temperatures above 30 °C (Table 1).

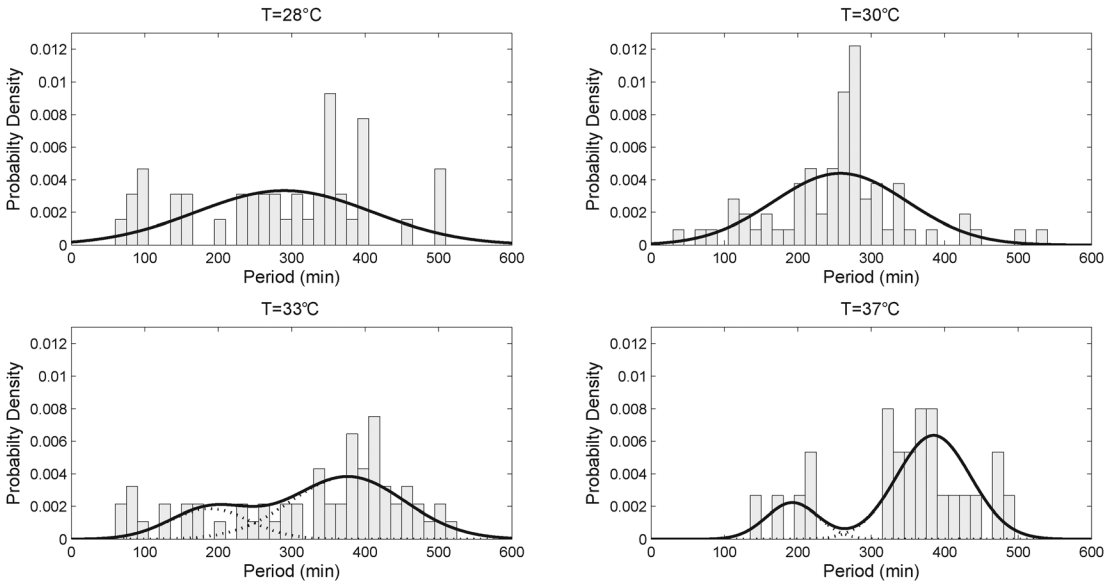

Fig. 4 Distribution of periods (magnitude scaled to represent probability density) for each temperature. Solid lines represent the probability densities of the fitted model with one or two Gaussians. Dashed lines represent the densities of individual components in the case of two Gaussians. For 28 °C and 30 °C, the p-values of the likelihood ratio tests are 0.08 and 1, respectively, indicating a lack of evidence for the two-Gaussian model, whereas for 33 °C and 37 °C, the p-values are 0.0065 and 0.0015, respectively, indicating that the two-Gaussian model should be favored over the one-Gaussian model.

Table 1 Kinetics of the repressilator at different temperatures. Temperature (T), fraction of functional cells (F), total number of cells exhibiting oscillations, fraction of robust oscillations (R), mean (m) and standard deviation (s) of the apparent period, and mean (μ) and standard deviation (σ) of the estimated true period are shown

T (°C)	F (%)	No. of cells oscillating	R (%)	m (min)	s (min)	μ (min)	σ (min)
28	20	43	100	290	120	290	120
30	30	71	100	258	91	258	91
33	15	62	26	328	126	188	59
37	5	25	20	347	92	192	36

Also in Table 1, we show the mean and standard deviation of both the apparent period and the true, estimated period. The mean true period, μ, always decreases with increasing temperature. On the other hand, the mean apparent period, m, is minimal at 30 °C.

Given this, we investigated whether the distributions of durations of true oscillations alone also differ with temperature, as the distributions of apparent oscillations do. Namely, we estimated the mean true period (Fig. 5) and then the one standard deviation of this estimate (error bars in Fig. 5). From Fig. 5, this mean always decreases significantly as temperature increases, except beyond 33 °C.

Next, we investigated the causes for the decrease in robustness with temperature. In particular, we investigated how temperature affects the functionality of the three component proteins of the repressilator, namely, CI, LacI, and TetR. First, studies suggest that as temperature increases from 30 °C to 42 °C, CI loses approximately half of its DNA-binding stability.[17] On the other hand, the DNA-binding affinity of LacI does not vary significantly between 28 °C and 37 °C.[27] Similarly, TetR's functionality is unaltered from 20 °C to 40 °C.[28] We thus hypothesized that a possible cause for the loss of robustness of the repressilator with increasing T was the weakening effectiveness of CI as a repressor.

There is another circuit, the CI–Cro genetic switch, of which CI is a component. If CI loses functionality with increasing temperature (partially or completely) the behaviour of this switch should change with temperature. To determine whether this is the case, we conducted *in vivo* measurements of RNA production, one event at a time, by one of the two genes of this switch. This particular gene is controlled by the promoter P_{RM}, and codes for CI as well as for a 48 MS2d binding array. The second gene of the switch, whose activity is not followed, is controlled by the promoter P_R and codes for Cro. Relevantly, Cro–DNA interactions do not vary significantly from 24–37 °C,[29] thus, behaviour changes in this switch with increasing temperature should mostly arise from the changes in CI–DNA interactions.

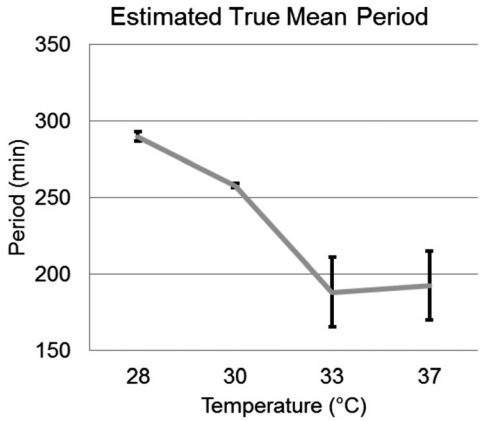

Fig. 5 Estimated mean values of the true period. Error bars indicate one standard deviations of the mean period estimated by the leave-one-out technique.

Table 2 Intervals between the appearances of novel, consecutive RNA molecules in individual cells. For condition, the table shows the number of intervals, mean (μ), standard deviation (σ) and, square of the coefficient of variation (CV^2) of the interval duration

T (°C)	No. intervals	μ (s)	σ (s)	CV^2
24	157	1242	1166	0.88
27	229	1452	1191	0.67
30	88	1130	1040	0.85
33	539	788	807	1.05
37	324	714	785	1.21

Table 3 *P*-values of the Kolmogorov–Smirnov test between distributions of intervals between consecutive RNA production events, under the control of P_{RM}, obtained at different temperatures. For *p*-values <0.01, the hypothesis that the two distributions are the same is rejected

T (°C)	24	27	30	33
27	0.149			
30		0.006		
33			0.009	
37				0.478

We measured intervals between consecutive productions of the RNA target for MS2-GFP in individual cells, from *in vivo* measurements 2 h long, with images taken every minute, at 24 °C, 27 °C, 30 °C, 33 °C and 37 °C. In Table 2, we show for each condition the number of samples (*i.e.* intervals) and the mean and standard deviation of the intervals' duration. As temperature increases, the kinetics of production of the target RNA changes. Specifically, aside from a decrease in the mean interval between consecutive transcription events, one observes that the production kinetics changes from sub-Poissonian ($CV^2 < 1$) for $T \leq 30$ °C, to super-Poissonian ($CV^2 > 1$) for $T > 30$ °C.

To verify if the change is significant, we compared the distributions of intervals in consecutive temperatures with the K–S test. The results in Table 3 indicate that the distributions at 24 °C and 27 °C cannot be statistically distinguished from one another. Similarly, the distributions at 33 °C and 37 °C cannot be distinguished. Meanwhile, the distributions from 27 °C and 30 °C, as well from 30 °C and 33 °C, differ from one another. Thus, there is a change in the dynamics of transcript production, and it occurs around 30 °C, which is similar to the point where changes in behaviour of the repressilator are observed.

Conclusions and discussion

We studied the behaviour of the repressilator at different temperatures. We observed that the fraction of functional cells

(*i.e.* exhibiting oscillations), the robustness of the oscillations in functional cells, and also the apparent and the real period all differ with temperature.

Because the robustness decreases at higher-than-optimal temperatures, the extraction of the period in this regime requires the identification of failed oscillations. Otherwise, the period will likely be overestimated. The extraction method here proposed should be applicable to other genetic clocks as well.

The apparent period was minimized at 30 °C. However, the results of employing the novel method of period extraction suggest that the increase in apparent period when increasing temperature beyond 30 °C is due to an increasing rate of failed oscillations. Meanwhile, the true period decreased significantly with increasing temperature (until 33 °C), in accordance with the response of other synthetic genetic clocks to increasing temperature.[30] This decrease is likely caused by the increased rate of the underlying thermodynamic processes (see ref. 30). In particular, we expect the decay rates of the proteins to increase, which decreases the period length.[35] The increased protein decay rates are expected from both increased rates of degradation and increased doubling rate of the cells. This allows the repressilator to be sensitive to temperature changes in the range tested.

We hypothesize that the design of genetic clocks that are insensitive to temperature will have to be able to compensate for increased speed of processes such as cell division, open complex formation,[13] among others.

Subsequently, based on previous studies on the functionality of the proteins of the repressilator,[17,27,28] we hypothesized that the loss of robustness with increasing temperature was associated with the temperature-dependent functionality of one component protein, CI. We tested this indirectly, by studying how temperature affects the CI–Cro switch. In particular, we conducted *in vivo* measurements, one event at a time, of the kinetics of production of an MS2-GFP tagged RNA that probed the transcription kinetics of the RNA coding for CI. From these, we observed that, when increasing temperature beyond 30 °C, the dynamics of production of the tagged RNA changed from sub-Poissonian to super-Poissonian, which suggests that the production of the tagged RNA became subject to repression.

Recent studies in *E. coli* suggest that, provided no repression, RNA production is a sub-Poissonian process, within the range of temperature tested here.[13,24,25,31] To be super-Poissonian, the promoter ought to have intervals of inactivity[21,34] (*e.g.* due to repressors) or due to another, similar mechanism. In the case of the CI–Cro switch, the occurrence of periods of inactivity of P_{RM} is expected if CI loses functionality, allowing Cro to be expressed.[32,33] Thus, these results suggest that CI loses functionality with increasing temperature.

The repressilator and the CI–Cro switch only share CI in common, while the other component proteins differ. Relevantly, the interactions between all these other proteins and their respective DNA binding sites are not temperature-dependent in the range studied.[27–29] Given this and all of the above, it is therefore reasonable to conclude that, in both circuits, the behavioural changes with temperature observed are primarily due to the temperature-dependence of CI's activity.[18,19]

Further, we hypothesize that it is possible to modify the repressilator so as to make it more robust to a wider range of temperatures. For that, the CI–DNA interaction should be replaced by a less temperature-dependent repression mechanism. This modification is not expected to compromise the sensitivity (which likely depends more heavily on the temperature-dependent cell division rate, among others).

It is worthwhile discussing the different effects of temperature on robustness and functionality. Namely, while functionality is maximized at 30 °C, robustness was only compromised at higher-than-optimal temperatures. In the latter regime, the two decreases are likely related. As robustness decreases, we expect a higher chance for repressilators to not function during the measurements. However, at lower-than-optimal temperatures, the loss in functionality is likely caused by other reasons, as the robustness was not compromised. Future research is needed to identify such causes.

Finally, the results presented here demonstrate that the behavioural changes in genetic circuits upon changing conditions depend not only on the topology of the circuit, but also on how each of its components responds to the environmental changes.

Acknowledgements

This work was supported by Academy of Finland (ASR), Finnish Funding Agency for Technology and Innovation (ASR), and Tampere City Science Foundation (AH). The funders had no role in study design, data collection and analysis, decision to publish, or preparation of the manuscript. We thank M. Elowitz and I. Golding for generously providing the genetic circuits.

Notes and references

1 C. H. Ko and J. S. Takahashi, *Hum. Mol. Genet.*, 2006, **15**, R271–R277.
2 Z. Neubauer and E. Calef, *J. Mol. Biol.*, 1970, **51**, 1–13.
3 D. L. Gally, J. A. Bogan, B. I. Eisenstein and I. C. Blomfield, *J. Mol. Biol.*, 1970, **51**, 1–13.
4 A. Becskei and L. Serrano, *Nature*, 2000, **405**, 590–593.
5 N. Nandagopal and M. B. Elowitz, *Science*, 2011, **333**, 1244–1248.
6 D. M. Wolf and A. P. Arkin, *Curr. Opin. Microbiol.*, 2003, **6**, 125–134.
7 M. B. Elowitz and S. Leibler, *Nature*, 2000, **403**, 335–338.
8 T. S. Gardner, C. Cantor and J. J. Collins, *Nature*, 2000, **403**, 339–342.
9 A. S. Khalil, T. K. Lu, C. J. Bashor, C. L. Ramirez, N. C. Pyenson, J. K. Joung and J. J. Collins, *Cell*, 2012, **150**, 647–658.
10 J. M. Callura, C. R. Cantor and J. J. Collins, *Proc. Natl. Acad. Sci. U. S. A.*, 2012, **109**, 5850–5855.
11 M. B. Elowitz and W. A. Lim, *Nature*, 2010, **468**, 889–890.
12 K. D. Litcofsky, R. B. Afeyan, R. J. Krom, A. S. Khalil and J. J. Collins, *Nat. Methods*, 2012, **9**, 1077–1080.

13 A.-B. Muthukrishnan, M. Kandhavelu, J. Lloyd-Price, F. Kudasov, S. Chowdhury, O. Yli-Harja and A. S. Ribeiro, *Nucleic Acids Res.*, 2012, **40**, 8472–8483.
14 D. M. Virshup and D. B. Forger, *Cell*, 2009, **137**, 602–604.
15 I. Mihalcescu, W. Hsing and S. Leibler, *Nature*, 2004, **430**, 81–85.
16 O. Oleksiuk, V. Jakovlejevic, N. Vladimirov, R. Carvalho, E. Paster, W. S. Ryu, Y. Meir, N. S. Wingreen, M. Kollmann and V. Sourjik, *Cell*, 2011, **145**(2), 312–321.
17 N. Jana, S. Roy, B. Bhattacharyya and N. C. Mandal, *Protein Eng.*, 1999, **12**(3), 225–233.
18 K. Koblan and G. Ackers, *Biochemistry*, 1991, **30**, 7822–7827.
19 K. Koblan and G. Ackers, *Biochemistry*, 1991, **30**, 7817–7821.
20 *Lambda II*, ed. R. W. Hendrix, J. W. Roberts, F. W. Stahl and R. A. Weisberg, Cold Spring Harbor Laboratory, Cold Spring Harbor, NY, 1983.
21 I. Golding, J. Paulsson, S. M. Zawilski and E. C. Cox, *Cell*, 2005, **123**, 1025–1036.
22 T. B. Chen, H. H. Lu, Y. S. Lee and H. J. Lan, *J. Biomed. Inf.*, 2008, **41**, 1021–1027.
23 N. Otsu, *IEEE Trans. Syst. Man Cybern.*, 1979, **9**, 62–66.
24 M. Kandhavelu, H. Mannerstrom, A. Gupta, A. Hakkinen, J. Lloyd-Price, O. Yli-Harja and A. S. Ribeiro, *BMC Syst. Biol.*, 2011, **5**, 149.
25 M. Kandhavelu, J. Lloyd-Price, A. Gupta, A.-B. Muthukrishnan, O. Yli-Harja and A. S. Ribeiro, *FEBS Lett.*, 2012, **586**, 3870–3875.
26 A. P. Dempster, N. M. Laird and D. B. Rubin, *J. R. Stat. Soc. Ser. B (Methodological)*, 1977, **39**(1), 1–38.
27 D. E. Frank, R. M. Saecker, J. P. Bond, M. W. Capp, O. V. Tsodikov, S. E. Melcher, M. M. Levandoski and M. T. Record Jr, *J. Mol. Biol.*, 1997, **267**, 1186–1206.
28 W. Hillen, G. Klock and I. Kaffenberger, *J. Biol. Chem.*, 1982, **257**, 6605–6613.
29 Y. Takeda, P. Ross and C. Mudd, *Proc. Natl. Acad. Sci. U. S. A.*, 1992, **89**, 8180–8184.
30 J. Stricker, S. Cookson, M. R. Bennet, W. H. Mather, L. S. Tsimring and J. Hasty, *Nature*, 2008, **456**, 516–520.
31 J. Mäkelä, M. Kandhavelu, S. Oliveira, J. Chandraseelan, J. Lloyd-Price, J. Peltonen, O. Yli-Harja and A. Ribeiro, *Nucleic Acids Res.*, 2013, **41**, 6544–6552.
32 L. Anderson and H. Yang, *Proc. Natl. Acad. Sci. U. S. A.*, 2008, **105**, 5827–5832.
33 S. Svenningsen, N. Costantino, D. Court and S. Adhya, *Proc. Natl. Acad. Sci. U. S. A.*, 2005, **102**, 4465–4469.
34 C. W. Gardiner, *Handbook of Stochastic Methods*, Springer, NY, 3rd edn, 2004.
35 A. Loinger and O. Biham, *Phys. Rev. E: Stat., Nonlinear, Soft Matter Phys.*, 2007, **76**, 051917.